NANO LETTERS

Letter

pubs.acs.org/NanoLett

Li Absorption and Intercalation in Single Layer Graphene and Few Layer Graphene by First Principles

Eunseok Lee* and Kristin A. Persson

Environmental Energy Technologies Division, Lawrence Berkeley National Laboratory, Berkeley, California 94720, United States

Supporting Information

ABSTRACT: We present an exhaustive first-principles investigation of Li absorption and intercalation in single layer graphene and few layer graphene, as compared to bulk graphite. For single layer graphene, the cluster expansion method is used to systemically search for the lowest energy ionic configuration as a function of absorbed Li content. It is predicted that there exists no Li arrangement that stabilizes Li absorption on the surface of single layer graphene unless that surface includes defects. From this result follows that defect-poor single layer graphene exhibits significantly inferior capacity compared to bulk graphite. For few layer graphene, we calibrate a semiempirical potential to include the effect of van der Waals interactions, which is essential to account for the contribution of empty (no Li) gallery to the total energy. We identify and analyze the Li intercalation mechanisms in few layer graphene and map out the sequence in stable phases as we move from single layer graphene, through few layer, to bulk graphite.

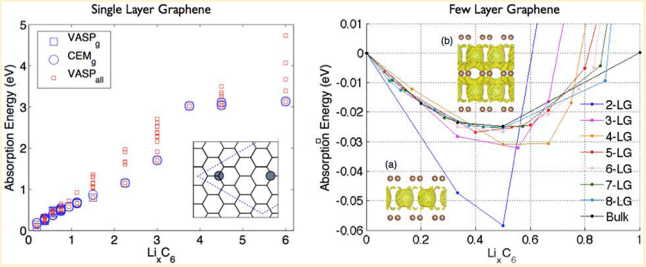

KEYWORDS: *Li-ion batteries anode, Graphene, Li absorption, Li intercalation, First-principles calculation, Cluster expansion method*

Today, rechargeable Li-ion batteries (LIB) present the leading energy storage technology solution for many applications from portable electronics to electric vehicle and grid storage. In commercial LIB systems, bulk graphite is the most widely used anode material due to its cost-effective performance.[1−5] Recent attempts to use the LIB in large capacity and high-rate applications have motivated research to find anode materials with superior performance metrics compared to graphitic carbons.

Since its discovery,[6] graphene, a single layer of honeycomb structured carbon atoms composing the bulk graphite, has attracted attention because of its ballistic electronic transport,[6] optoelectronic properties[7] as well as its unique two-dimensional geometry. In particular, some experimental[8−11] and computational[2,3,12−16] studies on the Li capacity of graphene are notable as they predict that graphene may absorb Li ions through a specialized Li ordering on both sides of the graphene, resulting in a higher theoretical capacity than graphite. However, there is conflicting experimental evidence that the Li capacity of graphene is significantly less than that of bulk graphite.[17] This controversy and the interest in graphene systems for electrode materials motivate a systematic study of Li absorption on single layer graphene as well as Li absorption and intercalation in few layer graphene.

In this paper, we perform a exhaustive investigation of the stability of Li-absorbed single layer graphene against the two-phase separation into a single layer graphene and metallic Li, using the cluster expansion method and density functional theory calculations. We also examine Li interactions, both absorption and intercalation, with few layer graphene to study how the Li-graphene system evolves from Li-graphene to Li-graphite. A semiempirical potential is calibrated to account for van der Waals interactions, which has a significant effect on the interactions between carbon atoms in neighboring graphene layers.

Single Layer Graphene. In bulk graphite, the Li ions are inserted into the space between two graphene layers (called gallery) and form $\sqrt{3} \times \sqrt{3}$ ordering (as illustrated in Figure 1a), which corresponds to LiC_6 and results in the maximum capacity of bulk graphite. For details on the Li absorption in the bulk graphite, see refs 1 and 5. However, in single layer

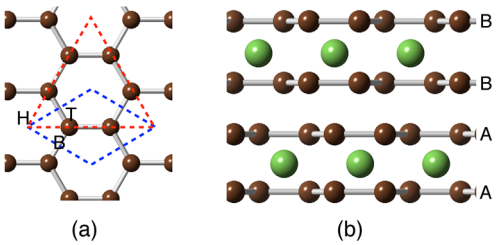

Figure 1. (a) Top view of a sigle layer graphene: primitive unit cell (blue dashed line), labeled three lattice sites for possible Li locations, and lattice sites for $\sqrt{3} \times \sqrt{3}$ Li ordering (red dashed line). (b) Side view of bulk graphite with stage II formation of Li: green, Li; brown, C.

Received: May 22, 2012
Revised: August 7, 2012
Published: August 24, 2012

graphene (SLG), the possibility of other Li orderings have been suggested due to graphene's unique geometric character and electronic properties.[2,3,12−16] Medeiros et al.[2] proposed that both sides of graphene can be used for Li absorption and predicted a corresponding Li ordering with one Li ion on the top of a carbon atom and another Li ion under the other carbon atom in primitive unit cell, resulting in a Li_6C_6 composition. Mapasha et al.[14] also suggested that Li ions can reside on the center of every carbon hexagon, resulting in Li_3C_6. To examine the feasibility of all possible Li orderings and resulting capacity of SLG, we employ a cluster expansion method (CEM) to systemically search and predict the ground state ionic configurations of the Li-absorbed SLG at any given Li content.

In the CEM, the ionic configuration of the Li-absorbed SLG can be mapped on a vector $\vec{\sigma}= (\sigma_1, \sigma_2,\cdots\sigma_N)$, where σ_i is +1 or −1 and indicates whether the lattice site i has Li or is empty. Thus the total energy of the system can be expanded with the σ_i as

$$E(\{\vec{\sigma}\}) = \sum_{\alpha} V_{\alpha} \prod_{i\in\alpha} \sigma_i \tag{1}$$

where V_α is called effective cluster interaction (ECI) for cluster α and is fitted to existing density funcational theory (DFT) data sets. Once the ECIs are fitted, eq 1 can be used to compute the energy of a new state, which is not included in the fitting. Since the number of DFT data sets need to be greater or equal to the number of ECIs for robust fitting, the clusters are grouped based on the translational and rotational symmetries to reduce the number of ECIs. For further truncation, a Monte Carlo algorithm is used to select relevant clusters by minimizing the cross-validation (CV) score. The ground state ionic configuration is converged through the iteration of fitting ECIs to existing DFT data sets and prediction of the lowest energy configuration, until the newly predicted configuration and its energy already exists in DFT data sets used in the fitting. We refer the reader to refs 18 and 19 for further details of the cluster expansion method.

We use a supercell consisting of a single layer graphene with 4 × 4 primitive cells and 15 Å vacuum space perpendicular to the graphene. When Li ions are absorbed on graphene, three lattice sites have been suggested for the possible position of Li ions as indicated in Figure 1a. Each primitive cell has 12 lattice sites for Li absorption (6 sites on each surface: one H, two T, and three B in Figure 1a). Perdew−Burke−Ernzerhof parametrization of the generalized gradient approximation[20,21] and projector augmented wave (PAW)[22,23] potentials as implemented in Vienna ab initio simulation package (VASP).[24−27] The 9 × 9 × 1 of k-points sampling is used with the cut off energy of 400 eV. The iteration of fitting-predicting converged after 87 DFT calculations with resulting CV score of 8 meV/C and an root-mean-square error of 7 meV/C. The absorption energy on a graphene sheet is defined as

$$E_a(x) = E(x) - E(0) - xE_{Li} \tag{2}$$

where $E(x)$ is the total energy of the system per one formula unit (FU), Li_xC_6, and E_{Li} is the energy of one metallic Li atom. Hence, the absorption energy examines the stability of Li-absorbed SLG against its phase separation into the stable end members: pure SLG and metallic Li. The absorption energy calculated from the converged CEM prediction is shown in Figure 2. We find that the absorption energy is positive in the entire range of the studied Li content and there exists no Li ordering with negative absorption energy, which contradicts previous theoretical predictions.[2,3,12−16] We ascribe the discrepancy between our prediction and the others to the use of different Li reference states. The correct reference state should be the stable bulk phase, as in a Li-ion battery; Li metal can form and indeed does at favorable potentials. (If a neutral Li gas atom is used as reference state, we indeed find some Li orderings with negative absorption energy in agreement with other computational predictions.) The strongest ECI corresponds to the point cluster of Li on the center of carbon hexagon. The most influential pair cluster corresponds to the longest pair used in the cluster expansion fitting and has negative ECI, which signifies strong repulsion between the Li ions at overlithiation.

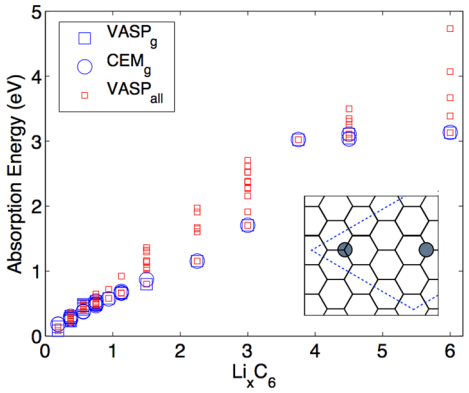

Figure 2. Absorption energy predicted by the DFT calculations ($VASP_g$,$VASP_{all}$) and the cluster expansion method (CEM_g) as a function of Li content, x. Subscript $_g$ and $_{all}$ indicate the data used in the last step iteration of the fitting-predicting procedure on convergence and all the data used through all the iterations, respectively. The inset illustrates the most influential pair cluster, which is the longest Li pair used in the cluster expansion fitting. The blue-dash line indicates the supercell.

Positive absorption energy for any Li content indicates that Li ions do not absorb on defect-free SLG, which renders it unsuitable for anode applications. Some experimental works report observations of Li-absorbed SLG, although their measurement of Li capacity ranges from Li_2C_6 to $Li_{0.3}C_6$.[8−10,17] We hypothesize that the Li absorption in those observations is due to the existence of defective microstructures and/or Li absorption on the graphene sheet edges. As an example, we found that an absorption energy of −0.21 eV/FU for one Li ion located on the top of carbon vacancy and −0.5 eV/FU for one Li ion attached to the edge of graphene.

Few Layer Graphene. We further investigate Li intercalation in few layer graphene (FLG). When multiple graphene layers are stacked, carbon atoms in two adjacent graphene layers are bonded by van der Waals (vdW) interactions. As Li ions intercalate into the galleries, the vdW bondings are perturbed and screened through the hybridization between the Li ions and carbon atoms.[5,10] Hence, the effect of vdW interactions on the Li intercalation into FLG can be significant and likely a function of the Li content as well as the number of graphene layers stacked together. However, standard DFT, specifically within the GGA, contains no vdW interaction and correspondingly exhibits no binding energy between the graphene layers, which is incompatible with experimental evidence. An excellent comparison between standard GGA/LDA and higher-order computational methodologies can be found in, for example, refs 28 and 29, for two-layer graphene

dx.doi.org/10.1021/nl3019164 | Nano Lett. 2012, 12, 4624−4628

and graphite. Since a vdW term is not included in the conventional Kohn−Sham equation form of DFT calculations, an additional functional needs to be included to account for the effect of vdW interactions. Two approaches are available for that purpose: one is the DFT-D2 approach, which adds a semiempirical pairwise force field to conventional DFT calculations,[30] and the other is the vdW-DF approach, which adds a nonlocal correlation functional that approximately account for dispersion interactions.[31,32]

We examine and benchmark these two approaches as implemented in VASP version 5.2.12 by changing their parameters to obtain the correct Li intercalation in bulk graphite as a function of Li content as obtained in previous computational work[5] where vdW interactions in bulk graphite are simply accounted for by incorporating a constant attractive energy correction for empty galleries. The supercell for bulk graphite is arranged to accommodate the $\sqrt{3} \times \sqrt{3}$ Li ordering and the sequence of stages. Each graphene layer contains 3×3 primitive cells, and the two adjacent graphene layers with/without Li intercalation between them are assumed to form AA (or BB)/AB stacking, respectively, as illustrated in Figure 1b. The interlayer distance is initially set to 3.5 Å, which will be adjusted by the vdW interaction during ionic relaxation. All ionic positions as well as the volume and shape of the supercell are allowed to change during the relaxation.

The benchmark result is shown in Figure 3. We observe that the intercalation energies (also defined as eq 2, but applied for

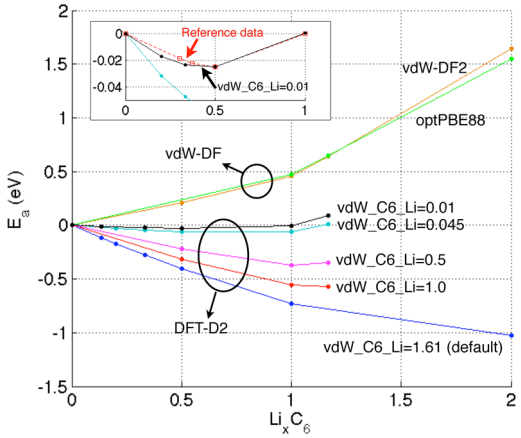

Figure 3. Benchmark result for the Li intercalation energy in the bulk graphite. Two approaches (vdW-DF and DFT-D2) accounting for the vdW interaction are examined. vdW_C6_Li indicates the dispersion coefficient for Li in the Grimme's semiempirical potential.[30] The subset figure shows a zoom-in comparison of the intercalation energy obtained in a previous computational work[5] and the results in this work using optimized parameters for DFT-D2.

the Li-intercalation) predicted by vdW-DF approaches (vdW-DF2 and optPBE88) deviate significantly from that of bulk graphite in previous work.[5] Since the vdW-DF methodologies obtain vdW interactions from the density, it is nontrivial to control the sensitivity of the parameters at the user-level. Instead, we focus on the DFT-D2 approach. Among several choices of parameter adjustments available, the best optimization occurs when the dispersion coefficient is 0.01 for Li and 1.75 (default) for C, as it demonstrates that the intercalation energy is negative at $0 < x < 1$, zero at $x = 1$, and positive (no Li intercalation) at $x > 1$, which is in agreement with experimental observations for the Li-graphite system.[33] (We focus on calibrating the dispersion coefficient for Li while maintaining the default values for C. For details, see the Supporting Information.) This optimization also correctly predicts the stage formation and voltage profile as a function of Li content, which is in agreement with the benchmarked reference data in previous computational work[5] and experimental data.[10] After the relaxation, the interlayer distance is found to be 3.50 Å for the Li-filled gallery (either AA or BB stacking) and 3.19 Å for the empty gallery (AB stacking). Although these values are underestimated as compared to the experimental values, 3.7 Å for AA (or BB) stacking and 3.35 Å for AB stacking, respectively, the trend and ratio of two interlayer distance are in agreement with experimental results.[1,5]

The optimized parameters are applied to investigate the Li intercalation into FLG as a function of the number of graphene layers (n). In the simulation, each graphene layer is composed of 3×3 primitive cells with 30 Å of vacuum space perpendicular to the graphene layers. Both the supercell shape and volume are relaxed during the ionic relaxation. A cutoff energy of 400 eV and $11 \times 11 \times 1$ of k-points sampling are used to ensure a high accuracy. To reduce the computational load, supercells are constructed so that the Li ions form the $\sqrt{3} \times \sqrt{3}$ ordering similar to bulk graphite. Two adjacent graphene layers with/without Li intercalation between them are assumed to form AA (or BB)/AB stacking, respectively, similar to bulk graphite. A few test cases of comparing the energy between AA (or BB) and AB stacking, such as 2−8 layers graphene with one Li filled gallery surrounded by two differently stacked graphene layers, were found to support this assumption.

The resulting intercalation energies for Li intercalated FLG as a function of Li content is shown in Figure 4. We find that Li

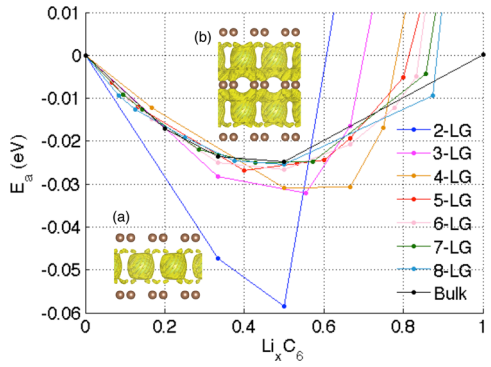

Figure 4. Li-intercalation in few layer graphene and the bulk graphite. For convenience, only the convex hull of intercalation energy is displayed. Subset figures show the charge transfer distribution in fully lithiated (a) bilayer and (b) trilayer graphene, using an isosurface level of 0.01.

can be intercalated in every n-LG (n layers graphene) and the Li intercalation is allowed only in the galleries, not on the surface, resulting in a Li capacity for n-LG of $(n-1)/n$ per C_6. Although $(n-1)/n$ per C_6 converges to 1 per C_6 with stacking more graphene layers, it implies that the Li capacity of FLG is inferior to that of bulk graphite. Interestingly, we find that the Li intercalation into bilayer graphene exhibits a much stronger intercalation for low Li content as compared to other FLGs, which manifests itself through a higher voltage. The Li intercalation in other FLGs uniformly converge to that of bulk graphite. The uniqueness of bilayer graphene, as compared

dx.doi.org/10.1021/nl3019164 | Nano Lett. 2012, 12, 4624−4628

to other FLG, has been observed in some experiments for FLG doped with other compounds such as NO_2 or Br_2.[34,35] We speculate that this uniqueness originates from the fact that the Li ions in bilayer graphene are surrounded by two exterior graphene layers, while the Li ions in other FLGs are always surrounded by at least one interior graphene layer. The charge transfer distribution, defined as $\rho - \rho_{graphene} - \rho_{Li}$, for the fully lithiated bilayer and trilayer graphene (see Figure 4) indicates that the bonding between Li and exterior graphene layers is more ionic than that between Li and interior graphenes, resulting in initially higher voltage for the bilayer graphene.

We further investigate how the Li−C phase changes with the number of graphene layers by examining the stable ionic configurations at each Li content. We find that when one Li ion intercalates into empty FLG, it prefers one of two outermost galleries (the galleries underneath the exterior graphenes) to the interior galleries in every n-LG. However, the subsequent Li intercalation behaves differently depending on the number of layers; Li ions can intercalate into the same outermost gallery, the other side outermost gallery, or interior galleries. We find that the behavior of Li intercalation can be categorized into the following two groups: (1) for $n \leq 6$, Li ions fill one outermost gallery fully, then fill the other outermost gallery fully, and then fill the interior galleries, and (2) for $n \geq 7$, Li ions fill both outermost galleries simultaneously and then fill the interior galleries.

The n-dependence of Li intercalation behavior filling the outermost galleries indicates the existence of interlayer Li−C interaction, which can also be inferred from the gallery width: when a Li ion is inserted into a gallery, the gallery width increases in the Li-intercalated gallery and decreases in the Li ion's nearest and the next nearest galleries while maintaining the original width in other galleries. Analysis of the charge distribution reveals that charge transfer between the intercalated Li ions and graphene layers is limited to the nearest neighbors. Hence, we speculate that the interlayer Li−C interaction indirectly manifests through the reconstruction between adjacent graphene layers due to the C−C vdW interactions. This interlayer Li−C interaction increases the total energy when Li ions in different galleries share any galleries within their interaction range. We can infer that this energy penalty is larger than the intralayer Li−Li repulsive interaction, because in the $n \leq 6$ FLG, fully filling the one outermost gallery is preferred to filling both outermost galleries simultaneously. When $n \geq 7$, Li ions in different outermost galleries have no shared galleries in their interaction range and hence Li ions intercalate both outermost galleries simultaneously.

In summary, we have elucidated the mechanism and strength of Li absorption in single layer graphene using the cluster expansion method and the density functional theory calculations. The predicted absorption energy for defect-free single layer graphene is positive for entire range of Li content, indicating that Li cannot reside on the surface of defect-free graphene which results in a theoretical Li capacity that is significantly inferior to that of bulk graphite. Furthermore, the Li intercalation in few layer graphene was studied, as a function of number of graphene layers, using additional functionals to account for van der Waals interaction. We found that few layer graphene systems intercalate Li ions but their capacity is still below that of bulk graphite. Our findings also show that the interaction between the intercalated Li ions and graphene layers propagates through the C−C interaction and ranges to the third nearest graphene layers. This complex multilayer interaction governs the Li intercalation sequence and phase formation in few layer graphene as a function of Li content and the number of layers.

■ ASSOCIATED CONTENT

Ⓢ Supporting Information

Additional information and figures. This material is available free of charge via the Internet at http://pubs.acs.org.

■ AUTHOR INFORMATION

Corresponding Author

*E-mail: eunseoklee@lbl.gov.

Notes

The authors declare no competing financial interest.

■ ACKNOWLEDGMENTS

Work at the Lawrence Berkeley National Laboratory was supported by the Assistant Secretary for Energy Efficiency and Renewable Energy, Office of Vehicle Technologies of the U.S. Department of Energy, under Contract No. DE-AC02-05CH11231.

■ REFERENCES

(1) Dresselhaus, M. S.; Dresselhaus, G. *Adv. Phys.* **2002**, *51*, 1−186.
(2) Medeiros, P. V. C.; de Brito Mota, F.; Mascarenhas, A. J. S.; de Castilho, C. M. C. *Nanotechnology* **2010**, *21*, 115701.
(3) Yang, C.-K. *Appl. Phys. Lett.* **2009**, *94*, 163115.
(4) Wang, X. *Appl. Phys. Lett.* **2009**, *95*, 183103.
(5) Persson, K.; Hinuma, Y.; Meng, Y. S.; der Ven, A. V.; Ceder, G. *Phys. Rev. B* **2010**, *82*, 125416.
(6) Novoselov, K. S.; Geim, A. K.; Morozov, S. V.; Jiang, D.; Zhang, Y.; Dubonos, S. V.; Grigorieva, I. V.; Firsov, A. A. *Science* **2004**, *306*, 666−669.
(7) Bonaccorso, F.; Sun, Z.; Hasan, T.; Ferrari, A. C. *Nat. Photonics* **2010**, *4*, 611−622.
(8) Wang, G.; Shen, X.; Yao, J.; Park, J. *Carbon* **2009**, *47*, 2049−2053.
(9) Lian, P.; Zhu, X.; Liang, S.; Li, Z.; Yang, W.; Wang, H. *Electrochim. Acta* **2010**, *55*, 3909−3914.
(10) Dahn, J. R.; Zheng, T.; Liu, Y.; Xue, J. S. *Science* **1995**, *270*, 590−593.
(11) Yoo, E.; Kim, J.; Hosono, E.; Zhou, H.-s.; Kudo, T.; Honma, I. *Nano Lett.* **2008**, *8*, 2277−2282.
(12) Chan, K. T.; Neaton, J. B.; Cohen, M. L. *Phys. Rev. B* **2008**, *77*, 235430.
(13) Khantha, M.; Cordero, N. A.; Molina, L. M.; Alonso, J. A.; Girifalco, L. A. *Phys. Rev. B* **2004**, *70*, 125422.
(14) Mapasha, R.; Chetty, N. *Comput. Mater. Sci.* **2010**, *49*, 787−791.
(15) Gerouki, A.; Goldner, M. A.; Goldner, R. B.; Haas, T. E.; Liu, T. Y.; Slaven, S. *J. Electrochem. Soc.* **1996**, *143*, L262−L263.
(16) Zheng, J.; Ren, Z.; Guo, P.; Fang, L.; Fan, J. *Appl. Surf. Sci.* **2011**, *258*, 1651−1655.
(17) Pollak, E.; Geng, B.; Jeon, K.-J.; Lucas, I. T.; Richardson, T. J.; Wang, F.; Kostecki, R. *Nano Lett.* **2010**, *10*, 3386−3388.
(18) Sanchez, J.; Ducastelle, F.; Gratias, D. *Phys. A: Statistical Mechanics and its Applications* **1984**, *128*, 334−350.
(19) Fontaine, D. D. Cluster Approach to Order-Disorder Transformations in Alloys. In *Solid State Physics*; Ehrenreich, H., Turnbull, D., Eds.; Academic Press: New York, 1994; Vol. *47*, pp 33−176.
(20) Perdew, J. P.; Burke, K.; Ernzerhof, M. *Phys. Rev. Lett.* **1997**, *78*, 1396.
(21) Perdew, J. P.; Burke, K.; Ernzerhof, M. *Phys. Rev. Lett.* **1996**, *77*, 3865.
(22) Kresse, G.; Joubert, D. *Phys. Rev. B* **1999**, *59*, 1758.
(23) Blöchl, P. E. *Phys. Rev. B* **1994**, *50*, 17953.
(24) Kresse, G.; Furthmüller, J. *Comput. Mater. Sci.* **1996**, *6*, 15−50.

(25) Kresse, G.; Furthmüller, J. *Phys. Rev. B* **1996**, *54*, 11169.
(26) Kresse, G.; Hafner, J. *Phys. Rev. B* **1994**, *49*, 14251.
(27) Kresse, G.; Hafner, J. *Phys. Rev. B* **1993**, *47*, 558.
(28) Rydberg, H.; Dion, M.; Jacobson, N.; Schröder, E.; Hyldgaard, P.; Simak, S. I.; Langreth, D. C.; Lundqvist, B. I. *Phys. Rev. Lett.* **2003**, *91*, 126402.
(29) Rydberg, H.; Jacobson, N.; Hyldgaard, P.; Simak, S.; Lundqvist, B.; Langreth, D. *Surf. Sci.* **2003**, *532*−*535*, 606−610 (Proceedings of the 7th International Conference on Nanometer-Scale Science and Technology and the 21st European Conference on Surface Science).
(30) Grimme, S. *J. Comput. Chem.* **2006**, *27*, 1787.
(31) Dion, M.; Rydberg, H.; Schröder, E.; Langreth, D. C.; Lundqvist, B. I. *Phys. Rev. Lett.* **2004**, *92*, 246401.
(32) Klimeš, J. c. v.; Bowler, D. R.; Michaelides, A. *Phys. Rev. B* **2011**, *83*, 195131.
(33) Stevens, D. A.; Dahn, J. R. *J. Electrochem. Soc.* **2001**, *148*, A803−A811.
(34) Crowther, A. C.; Ghassaei, A.; Jung, N.; Brus, L. E. *ACS Nano* **2012**, *6*, 1865−1875.
(35) Jung, N.; Crowther, A. C.; Kim, N.; Kim, P.; Brus, L. *ACS Nano* **2010**, *4*, 7005−7013.

dx.doi.org/10.1021/nl3019164 | *Nano Lett.* 2012, 12, 4624−4628